Characterization of Flame Cut Heavy Steel – Modeling of Temperature History and Residual Stress Formation

T. Jokiaho[a,*,1], A. Laitinen[a], S. Santa-aho[a], M. Isakov[a], P. Peura[a], T. Saarinen[b,c], A. Lehtovaara[a], M. Vippola[a]

[a]Tampere University of Technology, Laboratory of Materials Science, P.O. Box 589, FI-33101 Tampere, Finland

[b]SSAB Europe Oy, Rautaruukintie 155, 92101 Raahe, Finland

[c]Sandvik Mining and Construction Oy, Pihtisulunkatu 9, 33330 Tampere, Finland[1]

*corresponding author

[1]tuomas.jokiaho@tut.fi

Abstract

Heavy steel plates are used in demanding applications that require both high strength and hardness. An important step in the production of such components is cutting the plates with a cost-effective thermal cutting method such as flame cutting. Flame cutting is performed with a controlled flame and oxygen jet, which burns the steel and forms a cutting edge. However, the thermal cutting of heavy steel plates causes several problems. A heat-affected zone (HAZ) is generated at the cut edge due to the steep temperature gradient. Consequently, volume changes, hardness variations and microstructural changes occur in the HAZ. In addition, residual stresses are formed at the cut edge during the process. In the worst case, unsuitable flame cutting practices generate cracks at the cut edge.

The flame cutting of thick steel plate was modeled by using the commercial finite element software ABAQUS. The results of modeling were verified by X-ray diffraction based residual stress measurements and microstructural analysis. The model provides several outcomes, such as obtaining more information related to the formation of residual stresses and the temperature history during the flame cutting process. In addition, an extensive series of flame cut samples was designed with the assistance of the model.

[1] Present address.

Keywords: flame cutting, heavy steel plate, finite element, heat-affected zone, temperature history, residual stress

Introduction

Flame cutting is a thermal cutting method generally used by steel manufacturers. It is an effective method for cutting thick wear-resistant steel plate, unlike mechanical cutting, which is both difficult and too slow for high production rates. Flame cutting is an exothermal process, which provides an advantage over other thermal cutting methods, because the heat generated from the cutting process supports the continuation of the flame cutting [1].

The flame cutting process consists of three steps. Firstly, the steel is heated locally to its ignition temperature by using a flame obtained from the combustion of a specific fuel gas mixed with oxygen. Secondly, the heated spot is burnt with a jet of pure oxygen, which creates a continuous chemical reaction between the oxygen and the steel. Thirdly, the oxygen jet not only burns the steel but also blows away the iron oxide that is formed during the cutting process. [2]

However, the flame cut edge is prone to cracking, which makes cutting of thick steel plate problematic. It has been shown [3] that an increase in both the hardness and thickness of the plate enhances the cracking tendency. Flame cutting produces a heat-affected zone (HAZ) at the cut edge of steel plate due to the generation of a steep thermal gradient during the cutting process. For example, Martín-Meizoso et al. [4] have reported that microstructural changes and hardness variations occur in the HAZ. Hardness values have been observed to be higher closer to the cut edge and decrease over a short distance from the cut edge [5]. In addition, the width of the HAZ decreases with increasing cutting speed [6]. Thomas et al. [7] found that flame cutting produces a martensitic layer on the steel edge. The thickness of the martensitic layer and the HAZ were observed to be dependent on the plate thickness and flame cutting speed.

The flame cutting process results in the formation of residual stresses in the cut edge of the steel. It has been reported [3] that high residual stresses in the cut edge promote crack formation. Residual stresses are formed by uneven plastic strains in the material which cause elastic strains. These elastic strains maintain the dimensional continuity in the vicinity of the plastically deformed regions [8]. The elastic strains and hence the residual stresses can be either compressive or tensile. Generally, residual compressive stresses are beneficial because they reduce the probability of cracking, whereas residual tensile stresses are unfavorable because they enhance it. Large thermal gradients produced by flame cutting cause residual stresses consisting both of thermal stresses and transformation stresses. Thermal stress arises from the inhomogeneous thermal expansion and contraction of the material, while transformation stress is produced by microstructural transformations and their different volumetric expansions. [9]

Several studies have been carried out to determine and model the generation of residual stresses during flame cutting. Wei et al. [10] modeled the flame cutting of 10-mm-thick steel plate and the simulation results indicated that a slower cutting speed produced a wider HAZ and more compressive stress than a faster cutting speed. However, the cutting speed did not have any notable impact on the residual tensile stress maxima. Thiébaud and Lebet [11] used the section method to measure the residual stress distribution from 60-mm-thick steel plate. The results indicated that there was a tensile stress region close to the cut edge, which decreased rapidly with increasing distance from the edge, and was partly balanced by a compressive stress region deeper in the subsurface. Thomas et al. [7] studied 25 mm and 35 mm steel plates and discovered that, at a short distance (0.1 mm) below the flame cutting edge, the stresses are compressive and deeper (>1 mm), the stresses are tensile. Lindgren et al. [3] measured and modeled the residual stresses produced by flame cutting 50-mm-thick steel plates and the simulation results indicated the formation of a low compression stress region close to the cut edge, which was followed by a high residual tensile stress region. The residual tensile stress state was lower in preheated samples compared to samples which were cut without preheating. This model was verified by using a hole drilling strain gauge method to measure the residual stresses from certain locations of the cut edge. Despite the earlier studies, the residual stress formation in thick wear-resistant steel plates during the flame cutting process remains a fairly unknown phenomenon. The effect of different cutting parameters has been studied to some extent but further information related to this topic is required.

The aim of this study was to develop a model, which provides an effective tool for investigating the flame cutting process of a thick wear-resistant steel plate. In addition, modeling creates an opportunity to obtain information about the steel plate during the flame cutting process, which is almost impossible to obtain experimentally. The present model enables us to systematically study the effect of different flame cutting parameters, such as various flame cutting speeds, cutting preheated plate and cutting steel plate of different plate thicknesses. In addition, with the assistance of the model we can design the flame cut parameters to be used in a comprehensive test series for future studies.

Material modeling and Experimental procedure

The modeling of the thick steel plate flame cutting process was carried out by using the commercial finite element software ABAQUS. The purpose of the modeling work was to simulate the behavior of a previously studied [12] low-alloyed wear-resistant steel, the composition of which is given in Table 1. In the preliminary study [12], the residual stress profiles were measured from some flame-cut thick wear-resistant steel plates. The modeled part here was a rectangular shape steel plate modelled as a two-dimensional plane strain section: the thickness (y-direction) was set to 40 millimeters and the width (x-direction) was defined as long enough that the body could be considered semi-infinite. The model was constructed with a mesh with over 33 000 four-node bilinear thermo-mechanically coupled elements (Fig.1). The mesh was designed to be denser (element size of 0.04 mm) in the middle section in order to ensure accurate results from the area of interest, which is the most critical for crack formation.

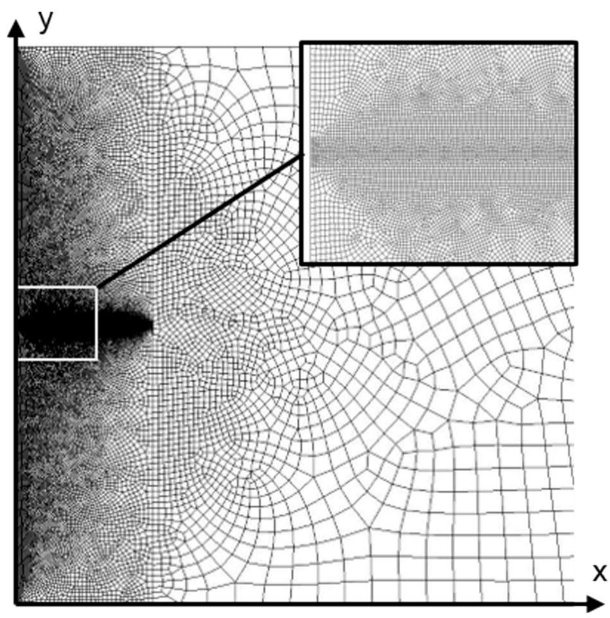

Fig. 1. *Finite element mesh with a zoomed view from the middle section.*

During the flame cutting process, every material point within the solid has its individual temperature history (i.e. maximal temperature, heating and cooling rate, etc.), which affects the material properties. For example, material properties during cooling depend on the maximum temperature attained during heating. Accurate simulation of these history effects would require a very large number of experimental tests and a large number of material parameters in the model. Therefore, in the model presented here a simplification is made, i.e. most of the thermal and mechanical properties are assumed to be directly temperature-dependent without any history effects. The only exception is the thermal expansion coefficients, which have different values depending on the maximum temperature and whether the part is heating up or cooling down. As explained below, thermal expansion coefficients are used to model the effect of phase transformations on a specific material volume. Therefore, a history-dependent approach is needed for these material properties. In order to acquire the temperature-dependent yield strength properties of the material, a series of uniaxial compression tests was conducted in various temperatures using a Gleeble 3800 thermo-mechanical simulator. The strain rate in the test was set to 1 1/s to correspond to the actual cutting process and the specimen was heated to the target temperature at a heating rate of 250 °C/s. Loading was applied for 0.5-1.0 seconds after reaching the target temperature, thus minimizing excess temperature effects like tempering.

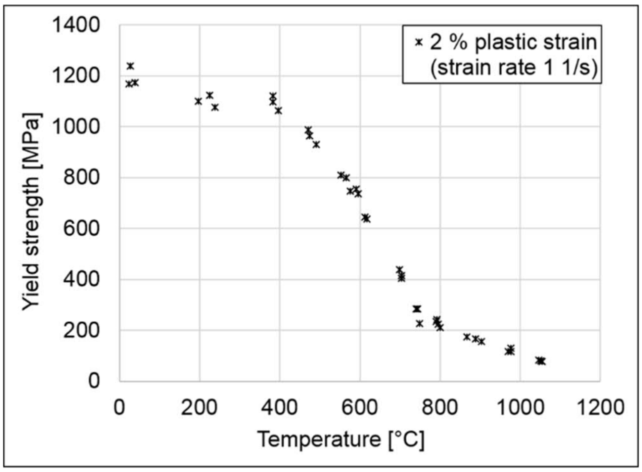

Fig. 2. *The results of the uniaxial compression tests using Gleeble: yield strength at 2 % plastic strain as a function of temperature.*

Fig. 2 shows that yield strength is a highly temperature-dependent material property and there is a significant drop in the yield strength values after the temperature rises above 400 °C. Acquiring correct values for yield strength as a function of temperature is important, since the yield limit decides whether the material reacts elastically or elastoplastically, which has a major impact on the stress distribution inside the steel plate. It should be noted that the yield strength values were measured for the heating stage only and assumed to adequately represent the material behavior also during the cooling stage.

In order to work correctly, the model requires phase transformation temperatures for both austenite (A_{c3} and A_{c1}) and martensite (M_s and M_f) transformations. Both the austenite start temperature (A_{c1}) and the martensite start temperature (M_s) were obtained using the Andrews equations [13]:

$$A_{c1}(°C) = 723 - 10{,}7Mn - 16.9Ni + 29.1Si + 16.9Cr + 290As + 6.38W \quad (1)$$

$$M_s(°C) = 539 - 423C - 30.4Mn - 17.7Ni - 12.1Cr - 7.5Mo \quad (2)$$

where the chemical symbols denote the weight percentage of the element in question. However, a different approach was needed for the full austenitizing temperature (A_{c3}), due to the rapid heating characteristic of flame cutting. The A_{c3} was set to 1077 °C after comparing the temperature distribution obtained from the model with microstructures observed from SEM micrographs, such as Fig. 3.

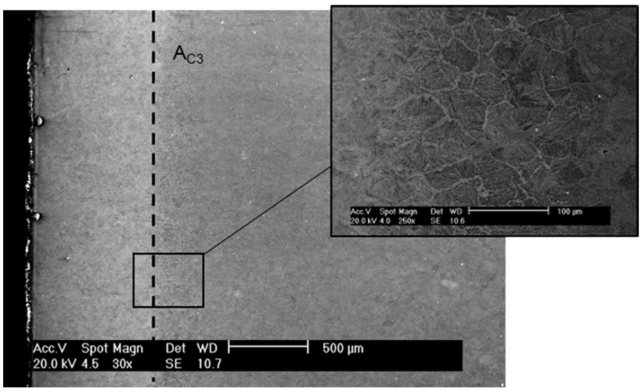

Fig. 3. *SEM micrograph from the cut edge of a 300 mm/min flame cut sample.*

In Fig. 3, the microstructural regions formed during the 300 mm/min flame cutting process can be seen. The fully martensitic region extends 0.8 mm from the flame cut edge of the sample. The M_f temperature was estimated to be 234 °C. According to Steven and Haynes [14], the M_f temperature can be approximated as 215 ± 15 °C below the M_s temperature. The phase transformation temperatures implemented in the model are shown in Table 2.

The thermal and phase transformation induced (austenite and martensite) volume changes were entered into the model as subroutines. The austenite phase fraction (f_a) was calculated using a modified Avrami function called Weibull's cumulative distribution function [15]:

$$f_a = f_{a_{final}} \left(1 - exp\left\{A\left(\frac{T - A_{c1}}{A_{c3} - A_{c1}}\right)^B\right\}\right), \quad (2)$$

where $f_{a_{final}}$ is the phase fraction at the end of the transformation, and A and B are material-dependent constants, set to -6 and 2, respectively [15]. The effect of austenite formation in the thermal axial expansion (ΔL/L) was calculated using the following equation:

$$\frac{\Delta L}{L} = (f_a \alpha_a + (1 - f_a)\alpha_s)\Delta T, \quad (3)$$

where α_s is the thermal expansion coefficient of the parent steel and α_a is the austenite thermal expansion coefficient, set to 13 x 10^{-6} 1/K and 20 x 10^{-6} 1/K, respectively. The thermal expansion coefficient of the martensite (α_m) was the same as that of the parent steel. The martensitic phase fraction (f_m) was calculated by using the equation derived from Koistinen and Marburger [16]:

$$f_m = 1 - exp\{\beta(M_s - T)\}, \quad (4)$$

where a value of -0.04 was used for β, which was selected so that 50 per cent of the martensite transformation happens almost instantly. The axial expansion changes caused by the martensitic phase transformation were introduced to the model via thermal expansion subroutines, as shown in the following equation:

$$\frac{\Delta L}{L} = \left\{f_a\left((1 - f_m)\alpha_a + (f_m \alpha_m) + \left(\frac{\Delta x_m}{x_m} / (M_f - M_s)\right)\right) + (1 - f_a)\alpha_s\right\}\Delta T, \quad (5)$$

where the $\Delta x_m / x_m$ is the axial expansion of the martensitic phase and was set to 0.75 per cent, which was evaluated to correspond to the real situation. The axial expansion can be converted to a volume expansion using the equation:

$$\frac{\Delta V}{V} = \left(1 + \frac{\Delta L}{L}\right)^3 - 1, \quad (6)$$

For simplification, the martensitic transformation was considered to be an isotropic volume expansion, which may not fully correlate with the actual martensitic transformation process.

The simulation of the flame is one step in the modeling of the flame cutting of a steel plate. From a modeling perspective, flame cutting is an extremely complex process with a large set of variables, which it is difficult to verify. However, the main purpose of this model was to study what occurs inside the steel when it is subjected to a large amount of heat, rather than the perfect modeling of the flame. Consequently, some simplifications had to be made. Therefore, the flame was created as a time-dependent heat flux, which simulated the movement of the flame. In the three dimensional preliminary simulations the flame was modeled as a moving line heat flux on the surface (the cutting surface) of the plate. Based on the results of these preliminary studies the heat source was modelled in the actual two-dimensional simulations as a heat flux boundary condition (Fig. 4(a)) on the edge on the element mesh (the left edge of the model in Fig.1). The movement of the flame was simulated by changing the amplitude of the flux with respect to time. Similar method has previously been used by Lindgren et al. [3]. To represent the real flame cutting process, the heat flux applied to the part was not totally uniform, thus the upper (flame) side of the part was subjected to more heat since the flame has a greater impact there. In addition, we used a time-dependent amplitude distribution of the heat flux in our model to resemble a moving flame. The amplitude distribution for the 150 mm/min cutting speed heat flux (Fig. 4(b)) was created by studying the data obtained from a simulation based on a three-dimensional flame model.

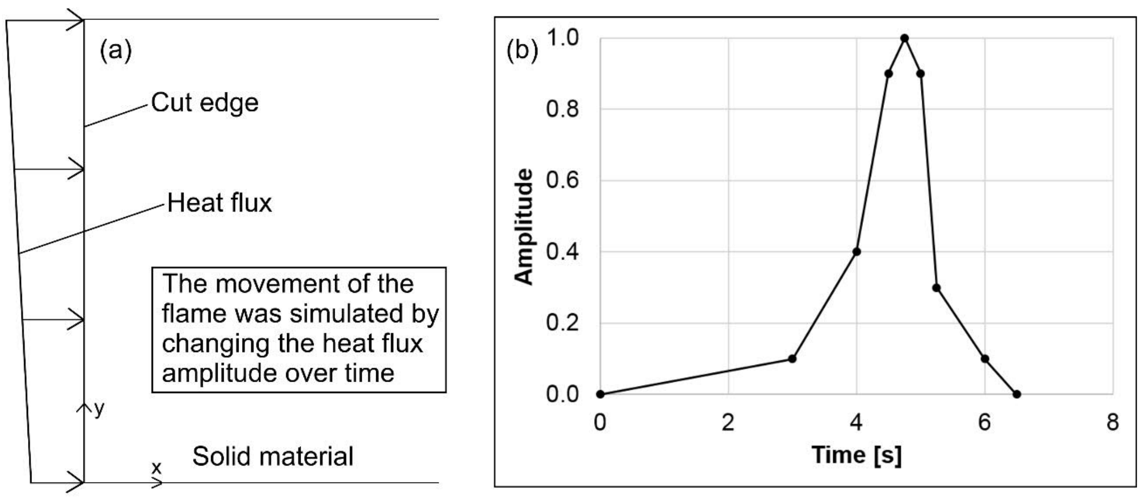

Fig. 4. *(a) Heat distribution along the cut edge (y-axis is the cutting depth). (b) The time-dependence of the heat flux amplitude for 150 mm/min cutting speed. It should be noted that the y-axis presents the magnitude of the heat flux relative to the maximum value.*

In Fig. 4(b), the time frame between 0 and 4.5 seconds simulates the heat transfer which occurs through conduction before the flame arrives. The period between 4.5 and 5 seconds simulates the moment when the flame is connected to the observed position. The time frame between 5 and 6.5 seconds represents the heat transfer to the observed position after the flame has passed. A similar heat flux amplitude was used for other cutting speeds, although the periods were divided according to how fast the process was compared to the 150 mm/min cutting speed.

The heat input for the flame was determined by iterating the magnitude of the heat flux. The heat input (maximum amplitude with reference to Fig. 4(b)) for thermal analysis was 1.8×10^7 W/m^2 and it was selected so that the surface temperature at the center of the plate (i.e., x=0 and y=0.5 x thickness in Fig. 1) reached the melting point of 1520 °C. The heat input for the stress analysis of 150 mm/min and 300 mm/min cutting speeds was set to 1.65×10^7 W/m^2 and 2.37×10^7 W/m^2, respectively. The heat flux for stress analysis was selected so that the maximum temperature at the above-mentioned location (surface of the center of the plate) was just below the melting point. This was necessary in order to avoid the removal of elements or setting them to zero, which would have an undesired effect on the analysis of the stress curves in the surface region. Since the heat flux represents the net heat, the heat losses of the flame are ignored. In addition, the model was used to study the effect of preheating, as it has been observed to lower tensile stress maximum values in residual stress measurements. Preheating was simulated by setting the modeled part for different predefined temperature fields and the heat flux magnitudes were adjusted so that the surface elements would not exceed the melting temperature.

The results of the model were verified by residual stress measurements done with an XStress 3000 X-ray diffractometer (manufactured by Stresstech Oy) and the measurement method used is called the modified Chi method [17]. This method calculates, using Bragg's law, the interplanar lattice spacing of the ferrite [211] plane from the 156° Bragg diffraction angle. The lattice plane spacing changes from a stress-free value to some new value depending on the magnitude of the residual stress. With this method, the lattice spacing d of the sample is measured at different ψ tilts, where the ψ angle is the angle between the normal of the sample and the normal of the diffracting plane. The measured values provide a slope containing a plot of lattice spacing d as a function of $\sin^2 \psi$. This slope with elastic constants can be used to calculate the residual stress from the measured location. Residual stresses are calculated using the following equation [18]:

$$\sigma = \left(\frac{E}{(1+\nu)}\right)m, \quad (7)$$

where the σ is the residual stress in the measured direction, E is the Young's modulus, ν is the Poisson's ratio and m is the slope obtained from the lattice spacing d vs. $\sin^2 \psi$ curve. The parameters used are listed in Table 3.

Residual stresses, used for model verification, were measured from 40-mm-thick samples, which were flame cut using cutting speeds of 150 mm/min, 300 mm/min and 300 mm/min with preheating at 200 °C. Samples were measured from two locations (A and B) and in two perpendicular measurement directions: the flame cut direction (0°) and the thickness direction (90°). These selected directions are the most critical orientations for crack formation. The measurement locations and directions are shown in Fig. 5.

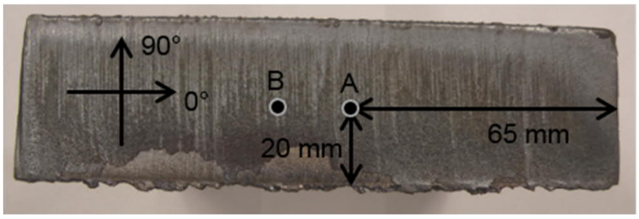

Fig. 5. *Residual stress measurement locations of X-ray diffraction method for a flame cut sample.*

Between the residual stress measurements, material layers were removed from the measurement location by electrochemical polishing. The polishing was done using Struers A2 electrolyte (a mixture of 60% perchloric acid, 65-85% ethanol, 10-15% 2-butoxyethanol and 5-15% water) and material removal was verified with a dial indicator. Residual stress measurement, combined with the layer removal method, provides residual stress depth profiles. The polished material depth was approximately 100-200 µm between each measurement. The measurement results were analyzed with XTronic software and residual stress profiles were plotted from the analyzed results.

Results and discussion

The model provided valuable information related to the temperature history of the part during the flame cutting process. Fig. 6 shows the modelled temperature profiles from different distances from the flame cut edge calculated at cutting speeds of 150 mm/min and 300 mm/min, respectively.

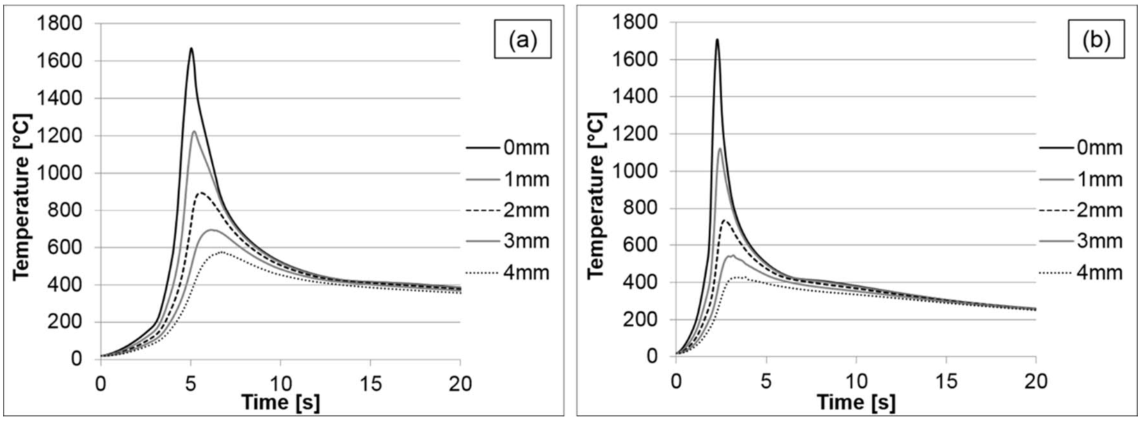

Fig. 6. *Temperature curves from different distances from the flame cut edge at (a) 150 mm/min and (b) 300 mm/min cutting speeds.*

Fig. 6 shows that the slower cutting speed creates more heat at the cut edge of the plate. In contrast, the faster cutting speed produces steeper thermal gradients compared to the slower cutting speed. With the slower cutting speed, the part has more time to heat up and the material has more time to adapt to the cutting situation. The shapes of the curves correspond to the experimental results of Thiébaud et al. [2].

One of the main purposes of the model was to reveal information on what occurs to the steel part during the flame cutting process. The uneven temperature distribution in the cut edge creates differing thermal expansion (and contraction) and consequently different residual thermal stresses. Fig. 7(a) shows the modeled thermal stress profiles (thickness direction) produced during the flame cutting process at cutting speeds of 150 mm/min and 300 mm/min. It should be noted that in general the maximum possible stress at a given temperature is limited by the current yield strength and fracture stress of the material, but in the simulations the plasticity of the material was taken into consideration. Therefore, the simulation results can be considered to indicate the best-case scenario, i.e. in reality, material fracture might take place at stress levels below those represented by the current simulations.

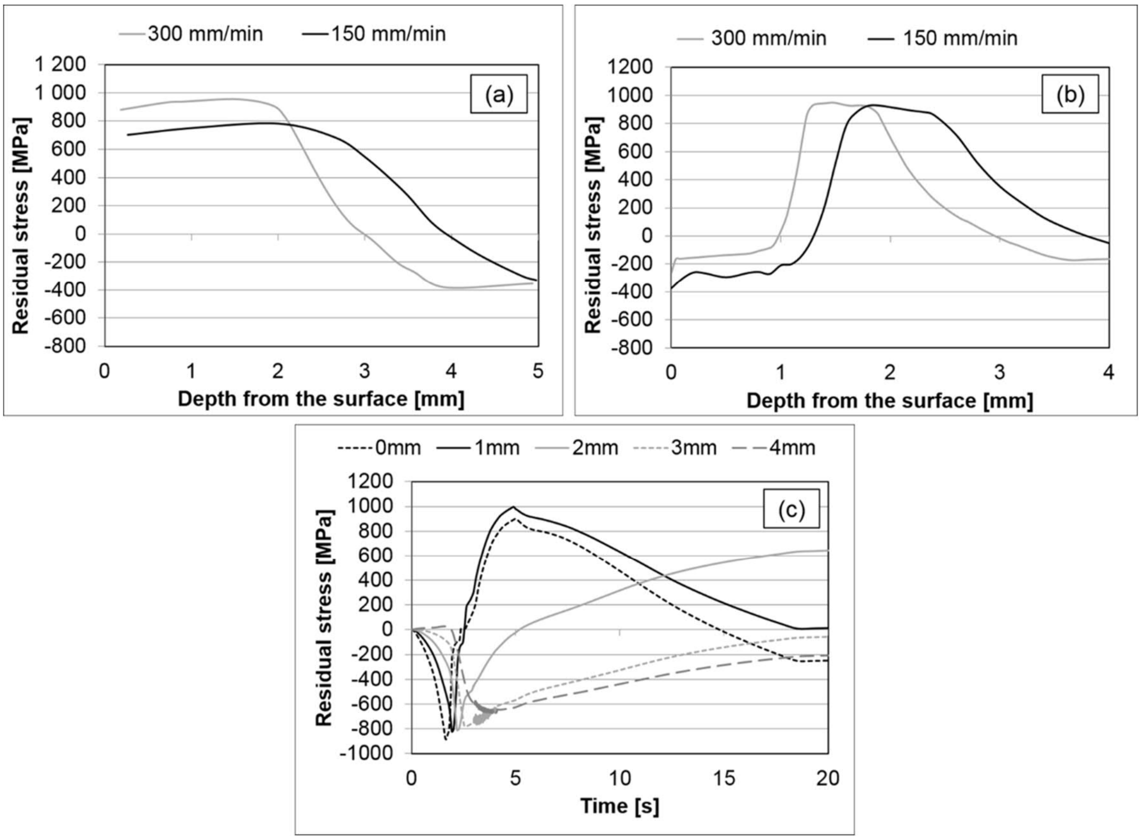

Fig. 7. *Simulated residual thermal stress profiles (thickness direction) of 150 mm/min and 300 mm/min flame cutting speeds (a) without phase transformations and (b) with phase transformations. (c) Modelled residual stress formation during flame cutting with 300 mm/min cutting speed.*

The residual thermal stress state during the flame cutting process is very difficult to determine experimentally; therefore, modeling is essentially the only tool capable of providing such information. In addition, simulations allow us to separate the effects of pure thermal expansion from the effects of phase transformations. This is illustrated in Fig. 7(a). Without the phase transformation, the residual thermal stresses are due to the uneven thermal expansion and contraction that occurs during cutting. The high temperature causes volume expansion in the cut edge, which is constrained by the cold surroundings, thus creating a compressive stress near the cut edge. Consequently, as the temperature increases and simultaneously the yield limit is lowered, the compressive stress exceeds the yield limit and produces a plastically deformed (compressed) region near the cut edge. During cooling, the contraction of the compressed region is restrained by the region without plastic deformation. For this reason, residual tensile stress is generated in the deformed region near the cut edge. The residual tensile stress is then balanced by the residual compressive stress deeper inside the part. As we can see from Figs. 6(a), 6(b) and 7(a), the faster cutting speed produces steeper thermal gradients in the cut edge, consequently creating higher thermal stresses in the cut edge compared to the slower cutting speed. Therefore, rapid and significant temperature changes should be avoided in the flame cut edge.

In the actual case, martensitic phase transformation is also involved in the steel structure during the flame cutting process. Fig. 7(b) shows the modeled residual stress profiles produced by 150 mm/min and 300 mm/min cutting speeds, which also takes into account the phase transformation. The effect of the volume expansion caused by martensitic transformation on the formation of the residual stress profiles is clearly seen. The martensitic transformation relieves the residual thermal tensile stresses near the flame cut edge and produces a residual compressive stress. The shapes of both residual stress curves are quite similar, but the residual compressive stress area at the surface is larger at the cutting speed of 150 mm/min than at 300 mm/min. The reason for this is the higher heat input caused by the slower cutting speed. Therefore, the phase transformation regions are larger and more elements experience the expansion effect due to martensitic transformation. Fig. 7(a) and 7(b) show that a cutting speed producing lower thermal stress also produces more residual compressive stress during martensitic transformation. This result also indicates that steep thermal gradients should be avoided during the flame cutting process.

Fig. 7(c) summarizes the whole chain of events that takes place during the flame cutting process. At first, the heat from the flame produces compressive stress near the surface. The stress changes to tensile once the heat is no longer applied and the part begins to cool down after 3 seconds. The tensile stress peak value is highest at 5 seconds, when the part has reached the M_s temperature and martensite starts to form, leading to volume expansion and hence to a change in the local stress state from tensile into compression. After the martensite transformation, the stresses gradually set into the final state (Fig. 7(b)) as the temperature decreases towards room temperature. The above-mentioned effect of martensite nucleation can be seen from the 0 mm and 1 mm stress curves, which are located in the phase transformation regions. However, the 2 mm curve is not located in the phase transformation region, and therefore the tensile stress continuously increases until the part reaches room temperature. Similar changes take place deeper in the material, but the resulting residual stress levels are at a lower level. It is noteworthy that, as Fig. 7(c) shows, the stress state near the surface changes during the cutting process (around 2.5 seconds in Figure 7c) from compressive stress to high tensile stress before changing back to compressive. This rapid change in the stress state takes place just prior to the martensitic transformation and might create potential sites for crack formation during the cutting process.

The model was used to predict residual stress formation with different flame cutting parameters and various plate thicknesses. Fig. 8 shows the residual stress curves for (a) different cutting speeds, (b) different plate thicknesses and (c) cutting at different preheating temperatures. The flame cutting speed of 300 mm/min was used in Fig. 8(b) and 8(c). The presented residual stress profiles are in the thickness direction of the modeled plate.

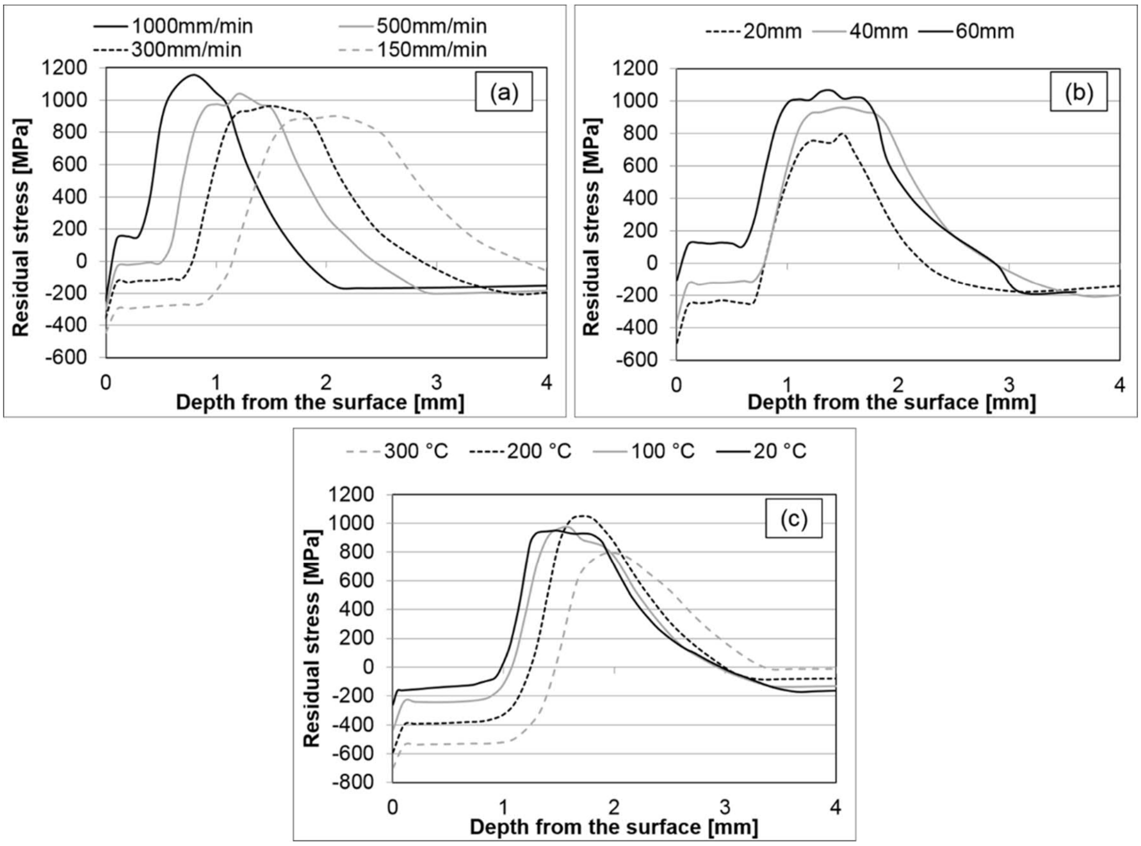

Fig. 8. *Simulation of the residual stresses (thickness direction) for different flame cutting processes: (a) cutting speed, (b) plate thickness, (c) preheating temperatures.*

Fig. 8(a) shows that there is a linear development in the residual stress profiles according to the cutting speed. The thermal shock effect from the flame is greater at faster cutting speeds; as a result, greater residual stress values are produced closer to the cut surface. The volume expansion of martensitic transformation is not enough to produce a residual compressive stress region on the surface at faster cutting speeds. These results also indicate that rapid heating should be prevented during flame cutting.

Fig. 8(b) shows the effect of plate thickness on the formation of residual stresses at a cutting speed of 300 mm/min. The vertical deformation is not as restricted in thinner plates as it is in thicker plates. Consequently, the cutting of thicker plates causes higher residual tensile stresses in the cut edge. In addition, the residual compressive stress decreases near the cut edge as the plate thickness increases. Therefore, due to the residual stress state produced by flame cutting, thicker plates are more prone to cracking than thinner plates.

As can be seen from Fig. 8(c), preheating lowers the residual stresses produced during flame cutting. Lindgren et al. [3] discovered similar effects with preheating compared to flame cutting without preheating. Preheating of the sample increases the residual compressive stresses and decreases the residual tensile stresses. However, present studies indicate that preheating not only increases the compressive stress but also expands the compressive stress region deeper in the subsurface. This is because the part is at a uniform preheating temperature; therefore, material deeper in the plate reaches the phase transformation temperatures when the heat is applied to the cut edge. Higher preheating temperatures decrease the effect of thermal shock by lowering the temperature differences inside the part, and consequently sufficiently high preheating temperatures decrease the residual tensile stresses.

Fig. 9 shows the modeled residual stress curve (thickness direction) (a) of 150 mm/min, (b) 300 mm/min and (c) 300 mm/min with 200 °C preheating, compared to experimentally measured data from a similar sample.

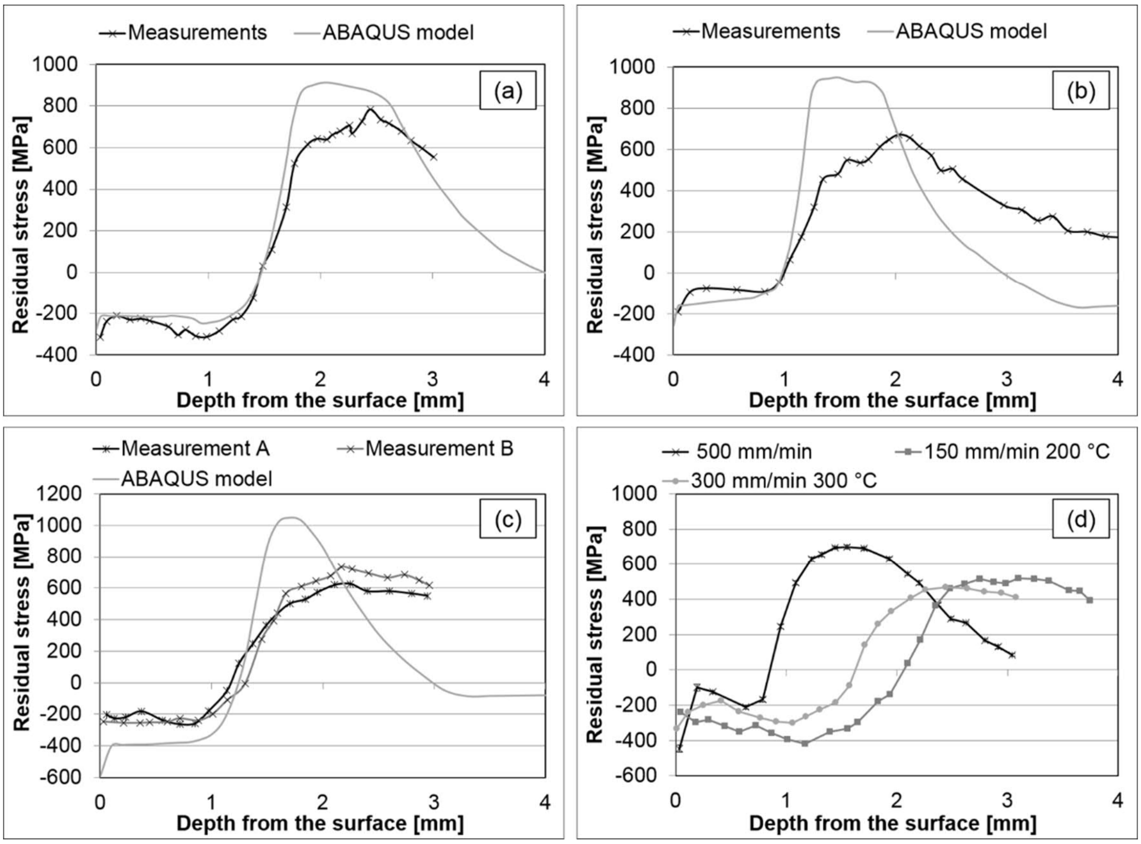

Fig. 9. *Comparison of modeled data with experimentally obtained data from (a) 150 mm/min, (b) 300 mm/min flame cutting speeds and (c) 300 mm/min cutting speed with 200 °C preheating. (d) Experimental measurements from samples which were flame cut using a cutting speed of 500 mm/min, 150 mm/min cutting speed with 200 °C preheating and 300 mm/min cutting speed with 300 °C preheating.*

Fig. 9(a) and 9(b) show that the compressive stress region is quite similar in both profiles; however, the residual tensile stress peaks are different. The tensile stress maximum is different in the model, which is to be expected, since the behavior of the material in the simulation is not totally equivalent to the behavior of steel in reality. The differences between the modelled and experimentally obtained residual stress curves of 300 mm/min (Fig. 9(b)) cutting speed are larger than for the 150 mm/min cutting speed (Fig. 9(a)). In the experimentally measured 300 mm/min flame cut sample, the tensile stress region is distributed to a larger area, which indicates that the material behavior and the heat load in the model are not fully accurate. Fig. 9(c) shows that preheating has a notable impact on the residual compressive stress region in both the modeled and measured profiles. However, there are differences, which can be explained by the slightly different cutting conditions in the actual flame cutting compared to the model. In addition, in the actual flame cutting, the tempering of martensite also occurs, which is not taken into account in the model. In the preheated sample there is more tempering during the flame cutting compared to that without preheating, which may also be a reason for the difference between measured and modeled data. In addition, it has been noted [19] that diffraction based residual stress measuring method not only measures the type I residual stresses (macrostresses over large distances) but the type II residual stresses (microstresses over grain scale) can be also superimposed in the results. The purpose of this work was to study only the generation of long range (type I residual stresses) stresses during flame cutting by finite element simulations. This difference might also cause the deviation between modeled and experimental results.

Perfect modeling of the flame cutting process is a challenging task and there are many variables. Consequently, there are some simplifications in the model, which might have an effect on the results. It should be noted that the cracking was not taken into account in the modeling. In addition, two-dimensional modeling involves some restrictions. For example, in actual flame cutting, the moving flame not only heats one side of the part but it also simultaneously heats the part from both the cut and approach directions. Furthermore, in the actual cutting process the solid part is still intact in front of the cutting flame, which may have an effect on the formation of residual stresses. To summarize the differences of the model and experimental results (Fig. 9(a), 9(b) and 9(c)), the main discrepancy is seen at depths of 1.5 mm and deeper. Based on Fig. 6, the material temperature in this depth reaches the two-phase region and the resulting final microstructure is therefore a mixture of transformed and non-transformed material. From simulation point of view, this is the most demanding region because of the following reasons: 1) The actual microstructure in this region is very sensitive to the temperature history, thus highlighting any uncertainties in the simulated temperature field. 2) As noted previously, the simulations involved some simplifications in terms of material behavior, the most notable of which was the use of one yield strength – temperature –curve (Fig. 2) for all metallurgical states of the material. This means that the plastic-deformation behavior in the above mentioned two-phase region is probably oversimplified. In addition, the yield strength data obtained from the Gleeble experiments is from the heating stage only and at the maximum temperature, which is lower than in the actual flame cutting process. 3) Some phenomena, such as tempering of the martensite, were left outside the scope of the simulations, which most likely influences the results deeper in the material (the temperature deeper in the material is high enough for a long enough time so that some tempering may take place). The tempering of steel during flame cutting has an effect on the volume of the tempered region. Therefore, the tempering also has an effect on the formation of residual stresses. In this respect, the correspondence between the simulations and the measurements is considered good.

In addition to the modeled results, Fig. 9(d) shows experimentally obtained residual stress profiles from samples which were flame cut using the following parameters: 500 mm/min cutting speed, 150 mm/min cutting speed with 200 °C preheating and 300 mm/min cutting speed with 300 °C preheating. It clearly shows how the residual stress state can be affected by different cutting parameters. The 500 mm/min cutting speed produces a high residual tensile stress peak but only a small amount of residual compressive stress near the cut edge. In contrast, the 300 mm/min cutting speed with 300 °C preheating produced significantly more residual compressive stress near the cut edge compared to cutting without preheating. The 150 mm/min cutting speed with 200 °C preheating also produced a similar kind of compressive stress region near the cut surface, although the compressive stress region extends deeper from the cut edge than the previous preheated sample. In addition, both preheated samples have a much lower tensile stress peak compared to the sample that was cut without preheating. These experimentally measured results confirm the predictions of the model: a slower cutting speed produces more residual compressive stress, lowers the residual tensile stress peak and preheating also has a similar effect on the residual stress state. In addition, the experimental measurements show that the widest compressive residual stress region and a significantly lower tensile stress peak can be produced by combining both a slow cutting speed and preheating. These results also confirm that the developed model gives accurate trend lines for evaluating residual stress formation during flame cutting.

Conclusions

Flame cutting of thick wear-resistant steel plates can be very problematic. It creates high residual stresses and may cause cracking of the steel plate. Consequently, a model was developed to investigate the problem and to study the flame cutting process. The model was created using the finite element software ABAQUS and the input material was made to behave as similarly to the studied steel as possible. The model takes into account the volume changes caused by thermal expansion (contraction) and phase transformation (austenite and martensite). A variety of simulations were computed using the model: flame cutting temperature histories, cutting at different cutting speeds, cutting different plate thicknesses and cutting using different preheating temperatures. The model enabled the study of residual stress formation during the flame cutting process, which would be extremely difficult or impossible to do experimentally. The results showed that the faster cutting speed produces steeper thermal gradients in the cut edge than the slower cutting speed and consequently higher residual tensile stresses. In addition, the slower cutting speed produced more residual compressive stress near the cut edge than the faster cutting speed. Therefore, rapid and large temperature variations during flame cutting should be avoided. In addition, the residual stresses vary quickly from compressive stress to tensile stress during the cutting process depending on the time and depth, which might create potential sites for crack formation. The results of the model also showed that varying the process parameters have an effect on the residual stress formation. The plate thickness also has an effect on the residual stress formation during the cutting process. Flame cutting of thinner plates created lower tensile stress maxima and more residual compressive stress than thicker plates. Therefore, the cracking tendency of thick plates is higher than thinner plates. The results also showed that preheating was an effective way to influence the residual stress formation during the cutting process. Flame cutting with preheating reduced the residual tensile stress and produced more compressive stress near the cut edge than cutting without preheating. In addition, the experimentally measured results confirmed the predictions of the model, as the slower cutting speed and preheating produced a wider residual compressive region and lowered tensile stresses. Additionally, the experimental results showed that combining both a slow cutting speed and preheating produced even more compressive stress and a significantly lower tensile stress peak. To conclude, the model produced valuable information about the flame cutting process and formation of residual stresses. In addition, the results of the model can be used as a basis for a new flame cut test series for future studies to reveal the comprehensive effect of microstructural features on residual stress and crack formation.

Acknowledgements

The funding for this work was mainly provided by the TUT graduate school. The authors would like to thank Mr. Juha Uusitalo from the University of Oulu for carrying out the Gleeble experiments.

References

[1] L.R. Soisson: 1993, ASM Handbook Online, ASM International, Vol. 6, pp. 1155-1165.

[2] R. Thiébaud, J. Drezet, J. Lebet: J. Mater. Process. Technol., 2014, vol. 214, pp. 304-310.

[3] L. Lindgren, A. Carlestam, M. Jonsson: J. Eng. Mater. Tech., 1993, vol. 115, pp. 440-445.

[4] A. Martín-Meizoso, J. Aldazabal, J.L. Pedrejón, S. Moreno: Frattura ed Integrita Strutturale, 2014, vol. 30, pp. 14-22.

[5] A.D. Wilson: Eng. J., 1990, vol. 27, pp. 98-107.

[6] W. Wood: Publ. No. FHWA-RD-93-015, U.S. Department of Transportation, Federal Highway Administration, Virginia, 1994.

[7] H. Thomas, J. De Back, T.J. Bos, T. Muller, J.J.W. Nibbering, C.J.J.M. Verwey, R. Vonk: Final report of Working Group 1913 of the Netherlands Institute of Welding, Technical Steel Research, Commission of the European Communities, Delft, 1980.

[8] G.S. Schajer: Practical Residual Stress Measurement Methods, 1 st. ed., John Wiley & Sons Ltd, Chichester, 2013, pp. 1-3.

[9] D. Radaj: Heat effects of welding: temperature field, residual stresses, distortion, Springer-Verlag, Berlin, 1992, pp. 7-9.

[10] Z.Y. Wei, Y.J. Liu, B. Zhou: Adv. Mat. Res., 2011, vol. 314-316, pp. 437-447.

[11] R. Thiébaud, J. Lebet: Experimental study of residual stresses in thick steel plates, Proceedings of the Annual Stability Conference Structural Stability Research Council, Texas, USA, 2012, pp. 1-16.

[12] T. Jokiaho, T. Saarinen, S. Santa-Aho, P. Peura, M. Vippola: Key Eng. Mater. 2016, vol. 674, pp. 103-108.

[13] K.W. Andrews: J. Iron Steel Inst., 1965, vol. 203, pp. 721-727.

[14] W. Steven, A.G. Haynes: J. Iron Steel Inst., 1956, vol. 183, pp. 349-359.

[15] S. Kamamoto, T. Nishimori, S. Kinoshita: Mater. Sci. Technol., 1985, vol. 1, pp. 798-804.

[16] D.P. Koistinen, R.E. Marburger: Acta Metall., 1959, vol. 7, pp. 59-60.

[17] SFS-EN 15305, Non-destructive Testing - Test Method for Residual stress analysis by X-ray Diffraction, 2008.

[18] M. Fitzpatrick, A. Fry, P. Holdway, F. Kandil, J. Shackleton, L. Suominen: International Measurement Good Practice Guide No. 52, Crown, 2005.

[19] P.J. Withers, H.K.D.H. Bhadeshia: Mater. Sci. Technol., 2001, Vol. 17, pp. 355-365.

Fig. 1. *Finite element mesh with a zoomed view from the middle section.*

Fig. 2. *The results of the uniaxial compression tests using Gleeble: yield strength at 2 % plastic strain as a function of temperature.*

Fig. 3. *SEM micrograph from the cut edge of a 300 mm/min flame cut sample.*

Fig. 4. *(a) Heat distribution along the cut edge (y-axis is the cutting depth). (b) The time-dependence of the heat flux amplitude for 150 mm/min cutting speed. It should be noted that the y-axis presents the magnitude of the heat flux relative to the maximum value.*

Fig. 5. *Residual stress measurement locations of X-ray diffraction method for a flame cut sample.*

Fig. 6. *Temperature curves from different distances from the flame cut edge at (a) 150 mm/min and (b) 300 mm/min cutting speeds.*

Fig. 7. *Simulated residual thermal stress profiles (thickness direction) of 150 mm/min and 300 mm/min flame cutting speeds (a) without phase transformations and (b) with phase transformations. (c) Modelled residual stress formation during flame cutting with 300 mm/min cutting speed.*

Fig. 8. *Simulation of the residual stresses (thickness direction) for different flame cutting processes: (a) cutting speed, (b) plate thickness, (c) preheating temperatures.*

Fig. 9. *Comparison of modeled data with experimentally obtained data from (a) 150 mm/min, (b) 300 mm/min flame cutting speeds and (c) 300 mm/min cutting speed with 200 °C preheating. (d) Experimental measurements from samples which were flame cut using a cutting speed of 500 mm/min, 150 mm/min cutting speed with 200 °C preheating and 300 mm/min cutting speed with 300 °C preheating.*

Table 1. *Chemical compositon approximation of studied steel.*

Amount of elements [Wt%]			
C	**Cr**	**Mn**	**Si**
0.130	0.890	0.970	0.620
Mo	**Al**	**Ni**	**B**
0.270	0.08	0.06	0.001
balanced with Fe			

Table 2. *Phase transformation temperatures implemented in the model.*

Temperature	Value [°C]	Value [K]
A_{c3}	1077	1350
A_{c1}	745	1018
M_s	440	713
M_f	234	507

Table 3. *Measurement parameters used for XStress 3000 equipment.*

Parameters:			
ϕ rotations (measurement directions)	0° and 90°	**Modulus of elasticity**	211 GPa
Collimator	3 mm	**Poisson's ratio**	0.3
ψ tilt angles in one direction (side / side)	6 / 6	**Voltage**	30 kV
Maximum tilt angle	40°	**Current**	6.7 mA
ψ oscillation	5°	**Radiation**	CrKα